Proceedings of the 20th International Conference on Soil Mechanics and Geotechnical Engineering– Rahman and Jaksa (Eds)

Simulation of damage evolution of cut-and-cover tunnels with 3D nonlinear finite element analysis

Duhee Park, Yonggook Lee
Department of Civil and Environmental Engineering, Hanyang University, South Korea
dpark@hanyang.ac.kr

Van-Quang Nguyen
Department of Civil Engineering, Vinh University, Vietnam

Bumjoo Kim
Civil and Environmental Engineering, Dongguk University, South Korea

ABSTRACT: The complex soil-structure interaction accounting for the nonlinear behavior of both the reinforced concrete and soil needs to be simulated for evaluation of the damage of cut-and-cover tunnels. We use the three-dimensional (3D) finite element (FE) model, where the concrete and steel rebars are modeled separately and assembled into a soil–tunnel model. The model is validated through comparison with the Daikai station case study, which collapsed during the 1995 Kobe earthquake. Simulation results illustrate that the 3D FE model is capable of reproducing the observed structural collapse. The cracks begin to form at the outer walls and propagate sequentially to the center column. The longitudinal and shear cracks in the center column induce a brittle loss of axial capacity. This type of failure cannot be captured by the plastic hinge model, most often used in practice.The damage evolution is revealed to be strongly correlated with the drift ratio of the center column.

RÉSUMÉ : L'interaction complexe entre sol et structure, découlant du comportement non-linéaire du béton armé et du sol, doit être simulée avec précision pour évaluer les dégâts sur l'évolution des tunnels en tranchée couverte. Nous utilisons le modèle d'éléments finis (EF) tridimensionnel (3D), où le béton et les armatures en acier sont modélisés séparément et assemblés dans un modèle sol-tunnel. Le modèle est validé par comparaison avec l'étude de cas de la station de Daikai, qui s'est effondrée lors du séisme de Kobe. Les résultats de la simulation montrent que le modèle EF 3D est capable de reproduire avec précision l'effondrement structurel et le tassement de surface. Les fissures commencent à se former sur les parois extérieures et se propagent séquentiellement jusqu'à la colonne centrale. Les fissures longitudinales et de cisaillement dans la colonne centrale induisent une perte fragile de capacité axiale. L'évolution des dommages est également fortement corrélée avec le taux de dérive de la colonne centrale. Les analyses démontrent qu'il est nécessaire d'incorporer un nouvel indice d'endommagement pour la prédiction de l'état d'endommagement des tunnels en tranchée couverte. Deux cas supplémentaires supplémentaires sont réalisés : soit avec un sol linéaire ou une structure linéaire. Au vu des résultats numériques, une analyses non linéaires est recommandée pour la simulations des dégâts.

KEYWORDS: damage evolution, collapse mechanism, soil-structure interaction, seismic analysis, underground structure.

1 INTRODUCTION

The tunnels are known to perform favorably during past severe seismic events compared with above-ground structures (Dowding 1978, Hashash et al. 2001, Arango 2008). However, the collapse of the Daikai subway station during the 1995 Kobe earthquake (Iida et al. 1996) and damages observed during the 1999 Chi-Chi earthquake (Wang et al. 2001) and 1999 Kocaeli earthquake (Ghasemi et al. 2000) reveal that even underground structures are vulnerable against severe seismic excitation. There is a need to understand the damage mechanism of underground structures and develop engineering indices to predict it. The Daikai station was adopted in this study because it is the only underground structure that has completely collapsed.

There were several studies to simulate the seismic response of the Daikai station. Due to the complex soil-structure interaction accounting for the nonlinear behavior of soil and reinforced concrete, three-dimensional (3D) FE numerical analyses have been mostly used for this purpose. Sayed, Kwon et al. (2019) employed the multi-platform simulation technique to analyze the Daikai subway tunnel that collapsed during the 1995 Kobe earthquake. The soil-tunnel system is subdivided into two substructures: the soil domain and the tunnel domain. The open-source finite element analysis program OpenSees (Mazzoni et al. 2007) is used to model equivalent linear behavior of the soil domain subjected to the ground motion excitation, while the state-of-the-art reinforced concrete analysis software package, VecTor2 (Wong et al. 2013), is used to model the nonlinear behavior of the tunnel. The two modules are integrated with the UT-SIM framework (Huang et al. 2015, Huang and Kwon 2020). The results replicated the crack pattern but tunnel did not collapse. Li and Chen (2017) developed a numerical model to investigate failure mechanism of Daikai station using Abaqus (ABAQUS 2012). A plastic damage model (Lubliner, Oliver et al. 1989, Lee and Fenves 1998), elasto-plastic model, and equivalent linear model were used for concrete, rebar, and soil, respectively. However, site-specific motion was not used and the structural damage pattern was different from the observation which failed in an “M” form. Ma et al. (2018) and Ma et al. (2018) also simulated the collapse of Daikai station using Abaqus (ABAQUS 2012). The models for concrete and rebar were used as in Li and Chen (2017). However, site-specific ground motion and soil profiles were not used. The literature review demonstrated that a study using a validated or verified numerical model to investigate the damage of tunnels has not yet been performed.

In this study, the collapse mechanism of the Daikai station was examined using 3D FE analysis. The concrete and rebar were model separately and assembled. An erosion model was used for the concrete to allow the spalling of damaged concrete. Effective index for predicting the level of damage of the underground structure is investigated.

2 FINITE ELEMENT MODEL

2.1 *Daikai tunnel structure model*

The tunnel section of the Daikai station has an outer dimension of 17.0 m width and 7.17 m height. The thickness of side walls is 0.7 m, while those of the top and base slabs are 0.8 m and 0.85 m, respectively. The clear height of the center column is 3.82 m with a cross-section of 0.4 m × 1 m, and the spacing between the columns is 3.5 m. Top and base slabs are connected to the column through beams with depths of 1.6 m and 1.75 m, respectively. The geometry and layout of steel rebars of the tunnel section are presented in Figure 1 and Figure 2, respectively. More details are available in Iida, Hiroto et al. (1996).

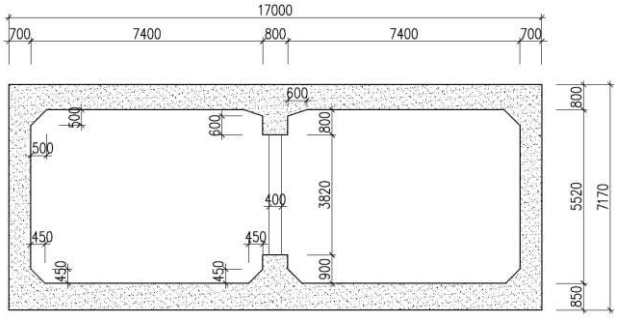

Figure 1. The geometry of the Daikai tunnel (all the dimensions are in millimeters).

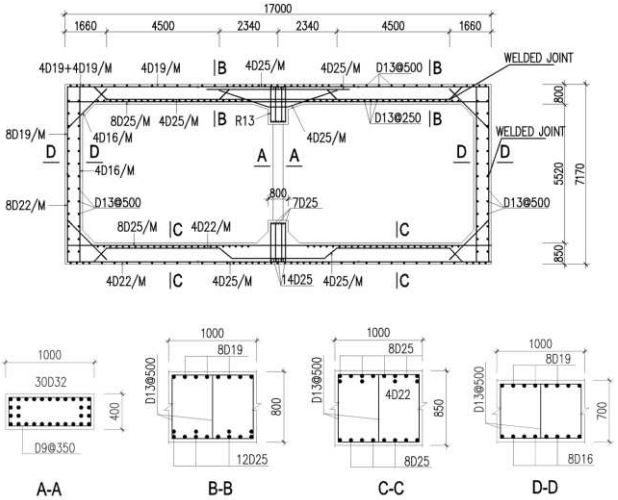

Figure 2. Reinforcement of the Daikai tunnel (all the dimensions are in millimeters).

A 3D FE model of the rectangular reinforced concrete tunnel lining was developed using LS-DYNA (Hallquist 2007), as depicted in Figure 3. The model depth is 3.5 m, which is equal to the spacing of the center column. Eight-node solid elements and beam elements are used to model concrete structure and steel rebar, respectively. The mesh size was 0.1 m for both the concrete and rebars.

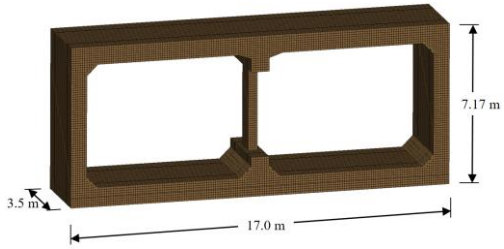

(a) Concrete

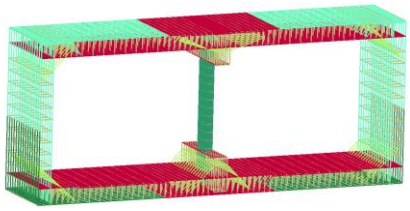

(b) Steel rebars

Figure 3. Type and mesh of finite element model.

In this study, the behavior of concrete was simulated using the Winfrith concrete model (MAT_084/085). The advantage of this model is the ability to simulate cracks. The model was reported to be applicable for dynamic applications (Coleman December 2016). The properties of concrete were adopted from (Iida et al. 1996, Li and Chen 2017, Ma et al. 2018) and listed in Table 1. Figure 4a presents the stress-strain relationship of the Winfrith concrete model. Moreover, a function of the element erosion was integrated with the concrete model. When the strain exceeds a given value, the element is removed from the computational model. The threshold limit was defined as the principal strain of ± 20%, consistent with the limits used in previous studies (Wilt et al. 2011, Bi et al. 2015, Thai and Kim 2017).

The kinematic hardening material model (MAT_003) was used to simulate the response of the steel rebars. The reinforcement is modeled as a beam element in the model. The failure strain at which the element erodes was set at 20%, based on the values used by Thai and Kim (2014), Omran and Mollaei (2017). Steel rebar properties were again adopted from Iida, Hiroto et al. (1996), Li and Chen (2017), and Ma et al. (2018) and listed in Table 2. The stress-strain relationship is shown in Figure 4b. The rebar-concrete contact was assumed to be fully bonded.

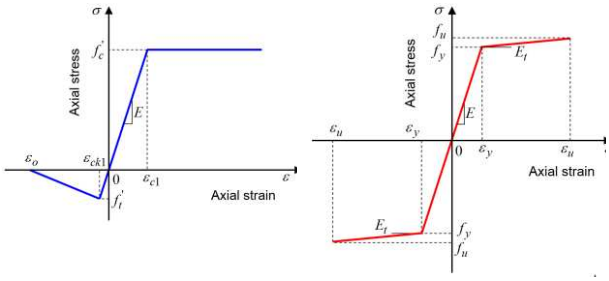

(a) Winfrith material model (MAT_084/085)

(b Kinematic hardening material model (MAT_003)

Figure 4. Stress-strain relationship of (a) concrete, (b) rebar.

Table 1. Concrete material properties.

Parameter	Value
Mass density (kg/m^3)	2500
Elastic modulus, E (GPa)	30
Poisson's ratio	0.18
Uniaxial compressive strength, f_c' (MPa)	49.6
Uniaxial tensile strength, f_t' (MPa)	3
Axial strain at compressive strength, ε_{c1} (%),	0.23
Axial strain at tensile strength, ε_{ck1} (%),	0.02
Ultimate strain value, ε_o (%)	0.14

Table 2. Reinforcement material properties.

Parameter	Value
Mass density (kg/m^3)	7800
Young's modulus, E (GPa)	200
Tangent modulus, E_t (GPa)	0.4
Poisson's ratio	0.3
Yield strength, f_y (MPa)	240
Yield strain, ε_y (%)	0.12
Ultimate strength, f_u (MPa)	320
Ultimate strain, ε_u (%)	20

2.2 *Soil domain model*

The site profile consists of 6 layers whose are presented in Figure 5, and the soil properties are listed in Table 3. The soil deposit of the Daikai station site is based on the report of Iida et al. (1996). The thickness of the soil profile used in the numerical analysis is 32 m.

Table 3. Soil properties.

No.	Material	Thickness (m)	Depth (m)	Density (kg/m^3)	Shear wave velocity (m/s)	Poisson's ratio
1	Fill	1.0	-1	1900	140	0.333
2	Pleistocene sand	4.1	-5.1	1900	140	0.488
3	Pleistocene sand	3.2	-8.3	1900	170	0.493
4	Pleistocene clay	3.1	-11.4	1900	190	0.494
5	Pleistocene clay	5.8	-17.2	1900	240	0.490
6	Gravel	14.8	-32	2000	330	0.487

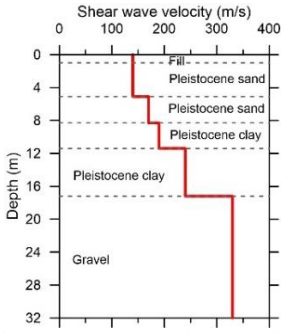

Figure 5. Stratigraphy and shear wave velocity profile.

The numerical model of the tunnel and soil domain is shown in Figure 6. The dimensions of the 3D computational model were set to 120 m × 32 m × 3.5 m (width × height × depth). The width of the soil domain was chosen based on sensitivity analyses conducted by the authors such that the waves reflected from the lateral boundaries have no effect on the seismic response of the tunnel. The spacing of the middle column is represented by the depth of the soil model. The soil element size was 0.5 m × 0.5 m × 0.5 m. The bottom boundary of the computational model was considered as the rigid base because the recorded motion from the vertical array was used (Kwok et al. 2007). Both the vertical and horizontal ground motions were imposed at the bottom boundary of the computational model. The free-field boundary condition at the lateral boundaries was simulated using equal degree-of-freedom constraints.

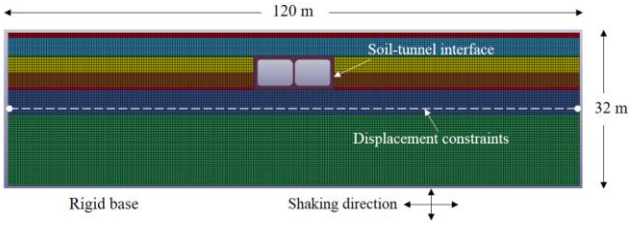

Figure 6. Numerical model of the tunnel and soil domain.

The nonlinear behavior of the soil was simulated using the hysteretic soil model (MAT_079). The model is composed of a series of parallel elastic-perfectly plastic materials to produce a nonlinear shear–stress curve (Bolisetti, Whittaker et al. 2018, Hashash, Dashti et al. 2018). The input properties of the nonlinear soil model were chosen such that the shear modulus reduction and damping curve fit favorably to the Darendeli target curves (Darendeli 2001) at the middle of each soil layer. Figure 7 compares the target and numerically calculated curves for layers 1, 2, and 4. The nonlinear soil model is shown to fit favorably to the target curves.

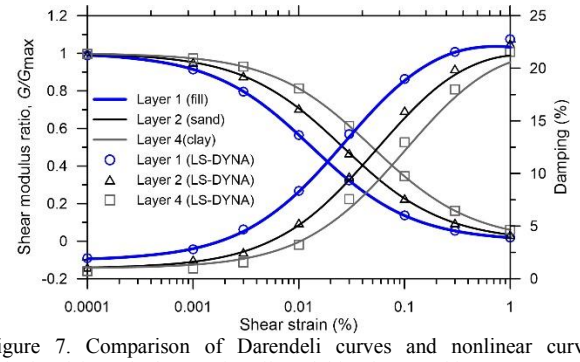

Figure 7. Comparison of Darendeli curves and nonlinear curves calculated from the hysteretic soil model implemented in LS-DYNA.

2.3 *Input motion*

The motion recorded at Port Island was used as the input because 1) Recording at Port Island is the closest to the Daikai station and 2) its soil profile is similar to that of the Daikai station site, as reported in Parra-Montesinos, Bobet et al. (2006). The north-south (N–S) and up-down (U–D) components recorded at a depth of 32 m were used as the input motions in the numerical simulation, as shown in Figure 8.

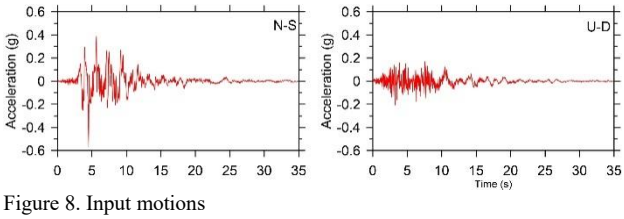

Figure 8. Input motions

3 RESULTS AND DISCUSSION

Figure 9 presents damage evolution of Daikai station from numerical analysis results at selected time step (t).

Figure 9a shows the response of the tunnel at t = 3.5 s, which the first crack formed. Horizontal cracks with widths of up to 2 mm are observed on the external walls. Subsequently, at t = 3.92 s, cracks occur at near the top and base of the center column, as shown in Figure 9b. Only the cracks exceeding 5 mm in width are shown in the figure. At t = 4.98 s, the first element erodes, as illustrated in Figure 9c. After the first erosion occurs, cracks are propagated wider at the bottom (Figure 9d) then to the top of the

center column (Figure 9e) and throughout the column. At t = 7.27 s, the loss of axial capacity causes the settlement of the top slab, inducing a significant concentration of bending moment. This results in the erosion of elements created at the right section of the top slab shown in Figure 9f. At t = 7.9 s, the top slab and the outer walls are severely damaged, represented by the erosion of more and more elements. No cracks are shown to develop at the base slab. A total collapse is observed at t = 8.21 s. The sequence of damage accumulation shows that the damage begins at the outer walls, but the center column causes the collapse of the tunnel. For this type of failure, reinforcement of the center column is critical to inhibit critical structural damage. The collapse pattern is almost identical to the observed damage (Iida et al. 1996). Another important observation is the type of cracks that develop in the center column. The longitudinal and shear cracks dominate in the column. This type of combined shear force and bending moment induced damage cannot be modeled by the fiber elements, which are most often used to model the reinforced concrete. An alternative procedure for estimating the damage of structural elements that have potentails for undergoing shear force motivated damage is warranted.

Figure 10 shows the drift ratios of the center column and the tunnel. The drift ratio of the center column is computed as the relative horizontal displacement divided by the apparent height of the center column. In contrast, the drift ratio of the tunnel is calculated as the ratio of the relative horizontal displacement of the outer wall to the total height of the tunnel. The damage evolution is linked to each peak of the drift ratio. At t = 3.5 s, the first crack is formed at the drift ratio of 0.44%. The center column damage is initiated at the drift ratio of 0.80% at 3.92 s, whereas the first erosion occurs at a drift ratio of 1.8% at 4.98 s. Noticeable tunnel damage occurs at a drift ratio of 1.80% for the center column corresponding to 0.93% for the tunnel. The observations demonstrate that it may be possible to use the drift ratio as a damage index to estimate the initiation of major damage state, in line with the damage evaluation of superstructure for which the interstory drift ratio is most often used. However, additional analyses are warranted to relate the drift ratio with specific damage states.

Two additional analyses were performed to investigate the pattern of drift ratio development. One analysis uses the linear soil and nonlinear structural models model, whereas the other analysis uses the nonlinear soil and linear structure models, respectively. For the linear models, elastic properties were applied. Figure 11 present the center column drift ratios (t = 5.2 s). The drift ratio for the case of linear soil model is lower than that for the linear structure model. It is noted that whereas the drift ratios at reversals increase for the baseline model incorporating both the nonlinear soil and structural responses, thereby capturing the accumulation of the damage of the tunnel structure, the drift ratios are shown not vary with time for two linear cases. Therefore, it is shown that use of the linear models to estimate the damge level from the drift ratio is not a viable option. Development of an alternative procedure to predict the damage level from simpler structrural model is warranted in the future even when using for routine application in practice.

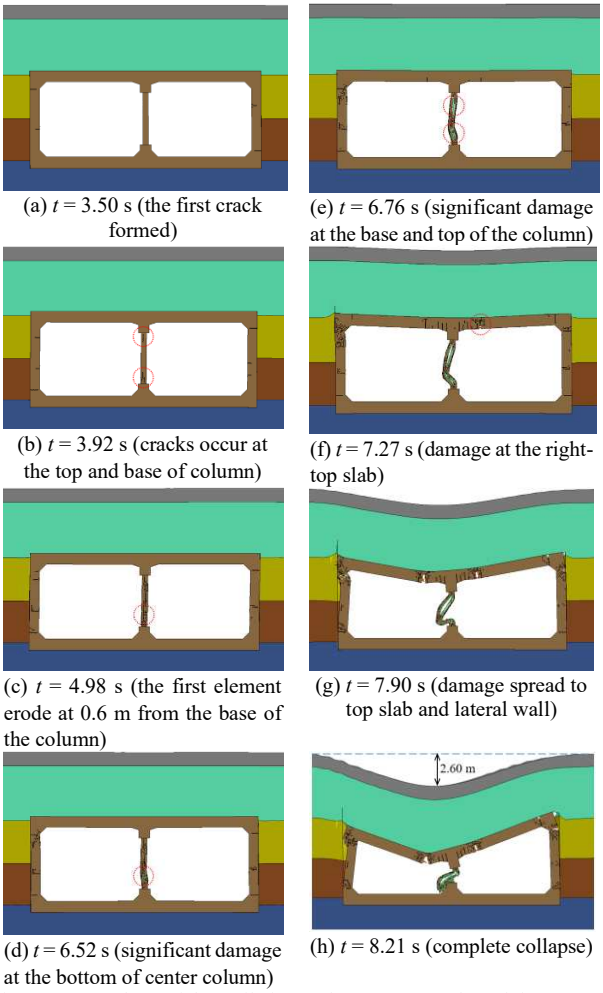

(a) t = 3.50 s (the first crack formed)
(e) t = 6.76 s (significant damage at the base and top of the column)
(b) t = 3.92 s (cracks occur at the top and base of column)
(f) t = 7.27 s (damage at the right-top slab)
(c) t = 4.98 s (the first element erode at 0.6 m from the base of the column)
(g) t = 7.90 s (damage spread to top slab and lateral wall)
(d) t = 6.52 s (significant damage at the bottom of center column)
(h) t = 8.21 s (complete collapse)

Figure 9. Snapshots of the Daikai tunnel response at selected time steps

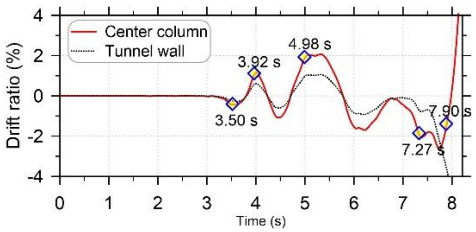

Figure 10. Tunnel/center column drift ratio history.

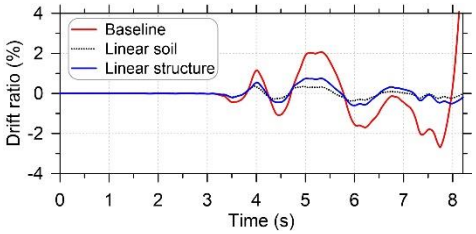

Figure 11. Comparison of the center column dirft ratio.

5 CONCLUSIONS

In this study, A 3D FE analysis was carried out for evaluation of the damage of evolution of Daikai station, which collapsed during the 1995 Kobe earthquake. Concrete and rebar steel were simulated separately and assembled. Bilinear and elasto-plastic models were used for concrete and rebars, respectively.

Moreover, an erosion model was used along with the nonlinear concrete model to capture the degradation of the strength and stiffness of concrete with the accumulation of structural damage. A nonlinear constitutive model was used for the surrounding soil.

Compare to observed damage (Iida et al. 1996), it revealed that using the site-specific soil profile and ground motion time records obtained during the Kobe earthquake, the nonlinear FE model is capable of correctly simulating the structure collapse. The pattern of the damage evolution was closely monitored to investigate the collapse mechanism. It was shown that cracks first appear at the outer walls, then in the middle column. Tensile and shear cracks occur and propagate over the whole column as ground motion intensity increases, causing considerable structural damage. When the axial capacity ò column is lost, the top slab settles significantly, and the tunnel collapses. It was noted that the structural collapse of the tunnel is strongly associated with the damage caused by the center collapse.

The time history of the drift ratio was extracted and compared with the accumulated damage. The significant structural damage of the center column occurs at a peak drift ratio of 1.8%. This finding suggests that the drift ratio may be utilized as a damage index to predict the level of damage in underground structures. Two additional analyses were performed to investigate whether the damage level can be estimated using either linear soil or structural models. It is shown that the accumulation of damage cannot be simulated, thereby demonstrating that the calculated drift ratio does not provide information on the damage level.

6 ACKNOWLEDGMENTS

This research was supported by a grant (18SCIP-B146946-01) from the Construction Technology Research Program funded by Ministry of Land, Infrastructure and Transport of Korean government.

7 REFERENCES

ABAQUS, C. 2012. Analysis user's manual, Version 6.12, ABAQUS.

Arango, I. 2008. Theme Paper: Earthquake Engineering for Tunnels and Underground Structures. A Case History. Geotechnical Earthquake Engineering and Soil Dynamics IV**:** 1-34.

Bi, K., W.-X. Ren, P.-F. Cheng and H. Hao 2015. "Domino-type progressive collapse analysis of a multi-span simply-supported bridge: A case study." *Engineering Structures* **90**: 172-182.

Bolisetti, C., A. S. Whittaker and J. L. Coleman 2018. "Linear and nonlinear soil-structure interaction analysis of buildings and safety-related nuclear structures." *Soil Dynamics and Earthquake Engineering* **107**: 218-233.

Coleman, D. K. December 2016. Evaluation of concrete modeling in LS-DYNA for seismic application. Master thesis Master thesis, The University of Texas at Austin, USA.

Darendeli, M. B. 2001. Development of a new family of normalized modulus reduction and material damping curves. Ph.D. Dissertation Ph.D. Dissertation, University of Texas at Austin.

Dowding, C. H. 1978. Seismic stability of underground openings. Storage in Excavated Rock Caverns: Rockstore 77, Elsevier**:** 231-238.

Ghasemi, H., J. D. Cooper, R. Imbsen, H. Piskin, F. Inal and A. Tiras 2000. "The November 1999 Duzce Earthquake: post-earthquake investigation of the structures on the TEM." *Rep. No. FHWA-RD-00* **146**: 00-146.

Hallquist, J. 2007. "LS-DYNA keyword user's manual, version 971 livermore software technology corporation."

Hashash, Y. M., S. Dashti, M. Musgrove, K. Gillis, M. Walker, K. Ellison and Y. I. Basarah 2018. "Influence of Tall Buildings on Seismic Response of Shallow Underground Structures." *Journal of Geotechnical and Geoenvironmental Engineering* **144**(12): 04018097.

Hashash, Y. M., J. J. Hook, B. Schmidt, I. John and C. Yao 2001. "Seismic design and analysis of underground structures." *Tunnelling and underground space technology* **16**(4): 247-293.

Huang, X. and O.-S. Kwon 2020. "A generalized numerical/experimental distributed simulation framework." *Journal of Earthquake Engineering* **24**(4): 682-703.

Huang, X., V. Sadeghian and O. Kwon 2015. "Development of integrated framework for distributed multi-platform simulation." *6AESE/11ANCRiSST, Champaign, IL*.

Iida, H., T. Hiroto, N. Yoshida and M. Iwafuji 1996. "Damage to Daikai subway station." *Soils and foundations* **36**(Special): 283-300.

Kwok, A. O., J. P. Stewart, Y. M. Hashash, N. Matasovic, R. Pyke, Z. Wang and Z. Yang 2007. "Use of exact solutions of wave propagation problems to guide implementation of nonlinear seismic ground response analysis procedures." *Journal of Geotechnical and Geoenvironmental Engineering* **133**(11): 1385-1398.

Lee, J. and G. L. Fenves 1998. "Plastic-damage model for cyclic loading of concrete structures." *Journal of engineering mechanics* **124**(8): 892-900.

Li, W. and Q. Chen 2017. "Seismic performance and failure mechanism of a subway station based on nonlinear finite element analysis." *KSCE Journal of Civil Engineering*: 1-12.

Lubliner, J., J. Oliver, S. Oller and E. Oñate 1989. "A plastic-damage model for concrete." *International Journal of solids and structures* **25**(3): 299-326.

Ma, C., D. Lu and X. Du 2018. "Seismic performance upgrading for underground structures by introducing sliding isolation bearings." *Tunnelling and Underground Space Technology* **74**: 1-9.

Ma, C., D. Lu, X. Du and C. Qi 2018. "Effect of buried depth on seismic response of rectangular underground structures considering the influence of ground loss." *Soil Dynamics and Earthquake Engineering* **106**: 278-297.

Mazzoni, S., F. McKenna, M. H. Scott and G. Fenves 2007. "The OpenSees command language manual, version 2.0." *Pacific earthquake engineering research center*.

Omran, M. E. and S. Mollaei 2017. "Assessment of empirical formulas for estimating residual axial capacity of blast damaged RC columns." *European Journal of Sustainable Development* **6**(3): 383-396.

Parra-Montesinos, G. J., A. Bobet and J. A. Ramirez 2006. "Evaluation of soil-structure interaction and structural collapse in Daikai subway station during Kobe earthquake." *ACI structural journal* **103**(1): 113.

Sayed, M. A., O.-S. Kwon, D. Park and Q. Van Nguyen 2019. "Multi-platform soil-structure interaction simulation of Daikai subway tunnel during the 1995 Kobe earthquake." *Soil Dynamics and Earthquake Engineering* **125**: 105643.

Thai, D.-K. and S.-E. Kim 2014. "Failure analysis of reinforced concrete walls under impact loading using the finite element approach." *Engineering Failure Analysis* **45**: 252-277.

Thai, D.-K. and S.-E. Kim 2017. "Numerical simulation of pre-stressed concrete slab subjected to moderate velocity impact loading." *Engineering Failure Analysis* **79**: 820-835.

Wang, W., T. Wang, J. Su, C. Lin, C. Seng and T. Huang 2001. "Assessment of damage in mountain tunnels due to the Taiwan Chi-Chi earthquake." *Tunnelling and underground space technology* **16**(3): 133-150.

Wilt, T., A. Chowdhury and P. Cox 2011. "Response of reinforced concrete structures to aircraft crash impact." *Prepared for US Nuclear Regulatory Commission Contract NRC-02-07-006*.

Wong, P., F. Vecchio and H. Trommels 2013. "Vector2 & Formworks user's manual second edition." *University of Toronto, Canada*.